Analysis and Control of STATCOM/SMES Compensator in a Load Variation Conditions

Mahmoud Reza SHAKARAMI[1], *Reza SEDAGHATI*[1], *Mohammad Bagher HADDADI*[2]

[1]Department of Electrical and Electronic Engineering, Engineering Faculty, Lorestan University, Daneshgat Street, 71234-98653 Khoramabad, Lorestan, Iran
[2]Department of Electrical Engineering, School of Engineering, Shiraz University, Bahar Azadi Street, 73159-88553 Kazeroon, Shiraz, Iran

shakarami@iust.ac.ir, reza_sedaghati@yahoo.com, haddadimohammadbagher@gmail.com

Abstract. *The utilization of Flexible AC Transmission System (FACTS) devices in a power system can potentially overcome limitations of the present mechanically controlled transmission system. Also, the advanced technology makes it possible to include new energy storage devices in the electrical power system. The integration of Superconducting Magnetic Energy Storage (SMES) into Static Synchronous Compensator (STATCOM) can lead to increase their flexibility to improve power system dynamic behavior by exchanging both active and reactive powers with power grids. This paper describes structure and behavior of STATCOM/SMES compensator in power systems. A control strategy based on direct Lyapanov method for compensator is used. Moreover, the performance of the STATCOM/SMES compensator in a load variation condition is evaluated by PSCAD/EMTDC software in test system. Also, SMES capacity effects on integrated compensator are investigated.*

Keywords

Direct Lyapanov method, load variation condition, SMES capacity, STATCOm/SMES compensator.

1. Introduction

In recent years, by ongoing growth in electric power demand and deregulation in the electrical power industry, numerous changes have been introduced to modern electricity industry. One of the most significant problems in power systems is that its power swings between synchronous generators and subsystems damped weakly and it must be controlled in appropriate way, otherwise the power system will encounter a significant problem and lose the conventional operation. Due to recent advances in high power semiconductor technology, FACTS technology has been proposed to solve this problem [1], [2].

Furthermore, as a typical FACTS device, STATCOM have been developed and utilized to improve transient stability margin, power quality improvement and damping power system oscillations by controlling reactive power [3], [4], [5]. Whereas significant increase in energy storage capacity for STATCOM lead to increase in degree of freedom and as a result its reliability and flexibility, therefore an energy storage system (ESS) for integration of STATCOM is proposed.

There are different technologies for energy storage such as ultra-capacitors, batteries, flywheels and SMES which the SMES system for power utility applications have received considerable attention due to rapid response, high power, high efficiency and four quadrant control [6], [7]. STATCOM and SMES are considered to cooperate and emerge as a compensator with prominent capability in power swings damping improvement. In [7] the SSSC/SMES application for frequency stabilization is examined and in [8] the experimental system integration of a battery energy storage system (BESS) into a STATCOM is discussed.

Specifically, this paper will present:

- Specifications and performance principles of the STATCOM/SMES compensator.
- Behavior of STATCOM/SMES in a load variation condition.
- SMES capacity effects on integrated compensator.

2. Proposed Model of Integrated STATCOM/SMES Compensator

A STATCOM can only absorb/inject reactive power, and consequently is limited in the degree of freedom. The STATCOM/SMES combination can provide a better dynamic performance than a stand alone STATCOM [7], [9]. A functional model of a STATCOM integrated with a SMES coil is shown in Fig. 1. This model consists main parts of the STATCOM controller, the SMES coil and the interface between both devices. The inclusion of a SMES in the dc bus of the STATCOM requires to adapt the voltage and current levels of both devices by utilizing an interface. In this case, a two-quadrant three-phase dc-dc converter is chosen as interface.

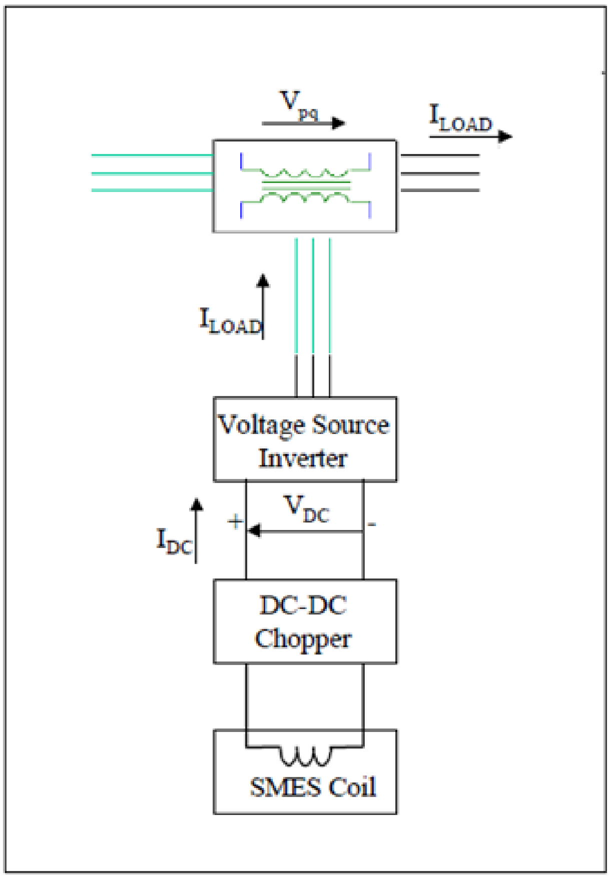

Fig. 1: General model of the integrated STATCOM/SMES compensator.

The chopper changes the dc current from the SMES coil to dc voltage, and a VSC changes the voltage into a three-phase ac current. Both the chopper and VSC need GTOs. The control of active and reactive powers was accomplished by controlling firing angles of the GTOs and the dc voltage that is determined by the duty ratio of the chopper. The angle and voltage differences between the utility line and the VSC output built current through the leakage inductance of the transformer that became the utility line current. The dc-dc chopper play in role of energy flow controller through the SMES coil [10]. When the SMES needs to be charged, the chopper connects the dc link voltage to the SMES so that the current inside the SMES increases and make a power flow from the dc link to the SMES coil. When the SMES needs to be discharged, the chopper connects the opposite voltage. The rate of charge/discharge is controlled by the voltage magnitude of the SMES coil. In other words, the dc-dc chopper changes the constant dc link voltage into a variable voltage required by the SMES coil to make the desired energy flow. Figure 2 shows a detailed configuration of the chopper. As shown in Fig. 2, the coil can be charged when the two GTOs are fired simultaneously and the diodes become reverse-biased. When both of GTOs are turned off, the coil discharges and the diodes become forward biased. At a duty cycle of 0.5, the SMES coil's average voltage and the VSC's average dc current are both zero, and no net power is transferred throughout one switching cycle. At a duty cycle larger than 0.5, the coil is charged; while at less than 0.5, the coil is discharged . Therefore, the control of charge/discharge process is accomplished by controlling the duty cycle [11].

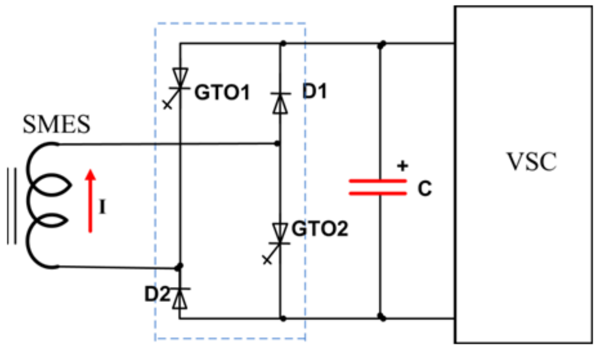

Fig. 2: Structure of a two-quadrant chopper.

3. Control Strategy for Integrated Compensator

3.1. Power System Model

Structure preserving model (SPM) of power systems has been presented to improve the modeling of generators and load representations such that system parts represent more realistic behavior [9]. Generators are modeled as one-axis generator model which includes one circuit for the field winding and also loads are modeled by constant active power and reactive power with following equations:

$$P_{Lk} = P_{Lk0}\left(\frac{V_k}{V_{k0}}\right)^{mp}, \quad Q_{Lk} = Q_{Lk0}\left(\frac{V_k}{V_{k0}}\right)^{mq}, \tag{1}$$

where P_{Lk} and Q_{Lk} will be the active and reactive powers at the nominal voltage Vo, respectively the P_{Lk} and Q_{Lk} real and reactive power of k-th load. mp and mq can be an arbitrary integer from 0 to 3. A power system with N buses and M generators without exciter and governor is considered. The system is assumed to be lossless. The governing equations of the system are:

$$\begin{aligned} &\dot{\delta}_i = \omega_i, \\ &M_i\dot{\omega}_i = P_{mi} - P_{Gi} - D_i\omega_i \\ &i = 1...M, \\ &T'_{doi}\dot{E}'_{qi} = \frac{x_{di} - x'_{di}}{x'_{di}} V_{M+i}\cos(\delta_i - \theta_{M+i} + \\ &+E_{fdi} - \frac{x_{di}}{x'_{di}}E'_{qi}), \end{aligned} \tag{2}$$

where ω_i and δ_i are velocity and mechanical angle of the i^{th} generator. M_i and D_i are inertia and damping factors for the i^{th} generator, x_{di} and x_{qi} are d and q-axis synchronous reactance of the i^{th} generator. T'_{doi} is the d-axis transient open circuit time constant of the i^{th} machine. E_{fdi} is the i^{th} generator exciter voltage, P_{mi} and P_{Gi} are the i^{th} generator mechanical and electrical power, respectively. Generated active and reactive electric powers are shown by:

$$\begin{aligned} &P_{Gi} = \frac{1}{X'_{di}}E'_{qi}V_{M+i}\sin(\delta_i - \theta_{M+i}) - \\ &-\frac{x'_{di} - x_{qi}}{2x'_{di}x_{qi}}V^2_{M+i}\sin(2(\delta_i - \theta_{M+i})), \\ &Q_{Gi} = \frac{1}{X'_{di}}\left[E'_{qi}V_{M+i}\cos(\theta_{M+i} - \delta_i) - V^2_{M+i}\right] + \\ &+\frac{x'_{di} - x_{qi}}{2x'_{di}x_{qi}}V^2_{M+i}\left[\cos(2(\theta_{M+i} - \delta_i) - 1)\right]. \end{aligned} \tag{3}$$

The injected real and reactive powers into k^{th} node are:

$$\begin{aligned} &P_k = \textstyle\sum_{i=M+1}^{M+N} B_{ki}V_kV_i\sin(\theta_k - \theta_i), \\ &Q_k = -\textstyle\sum_{i=M+1}^{M+N} B_{ki}V_kV_i\cos(\theta_k - \theta_i), \end{aligned} \tag{4}$$

where V_i and θ_i are the magnitude and phase voltage of the i^{th} bus, B_{ki} is the susceptance of the k -i branch. P_k and Q_k are the active and reactive power injected into k^h node. P_{Lk} and Q_{Lk} are active and reactive powers of k^h load.

Therefore, the equilibrium of powers at load buses offers the load flow equations as:

$$\begin{aligned} &P_k + P_{Lk} - P_{Gk} = 0, \\ &Q_k + Q_{Lk} - Q_{Gk} = 0. \end{aligned} \tag{5}$$

3.2. Direct Lyapanov Method

Let $w(x)$ be the direct Lyapunov function or energy function explained for the power system model described by Eq. (2) through Eq. (5). Any disturbance in power system involves a power imbalance that moves the system trajectory from the pre-fault stable equilibrium point to a transient point $x_i(t)$ that has a higher energy level than post-fault equilibrium point. If $\dot{w} = dw/dt$ is negative, direct Lyapunov function $w(x)$ decreases with time and tends towards its minimum value which appears at the post-fault equilibrium point $\hat{x}_i$. The more negative value of $\dot{w}$ means the system returns to the equilibrium point $\hat{x}_i$ quickly (i.e. the better damping in power system) [12], [13]. With assumption of $\hat{x}_i = 0$, the direct Lyapunov function for SPM power system without any control is written by:

$$\begin{aligned} &w(\omega, \delta, E'_q, V, \theta) = w_1 + w_2 + C_0, \\ &w_1 = \frac{1}{2}\textstyle\sum_{k=1}^{M} M_k\omega_k^2, \\ &w_2 = \textstyle\sum_{i=1}^{8} w_{2i}, \end{aligned} \tag{6}$$

where w_1 is kinetic energy and w_2 is potential energy that will be described as:

$$
\begin{aligned}
&w_{21} = -\sum_{k=1}^{M} P_{mk}\delta_{mk},\\
&w_{22} = \sum_{k=M+1}^{M+N} P_{Lk}\theta_k,\\
&w_{23} = \sum_{k=M+1}^{M+N} \int \frac{Q_{Lk}}{V_k} dV_k,\\
&w_{24} = \sum_{k=M+1}^{2M} \frac{1}{2x'_{dk-M}} [E'^2_{qk-M} + V_k^2 -\\
&-2E'_{qk} V_k \cos(\delta_{k-M} - \theta_k)],\\
&w_{25} = -\frac{1}{2} \sum_{k=M+1}^{M+N} \sum_{l=M+1}^{M+N} B_{kl} V_k V_l\\
&\cos(\theta_k - \theta_l),\\
&w_{26} = \sum_{k=M+1}^{M} \frac{x'_{dk-M} - x_{qk-M}}{4x'_{dk-M} x_{qk-M}}\\
&\left[V_k^2 - V_k^2 \cos(2(\delta_{k-M} - \theta_k))\right],\\
&w_{27} = -\sum_{k=1}^{M} \frac{E_{fdk} E'_{qk}}{x_{dk} - x'_{dk}},\\
&w_{28} = -\sum_{k=1}^{M} \frac{E'^2_{qk}}{2(x_{dk} - x'_{dk})}.
\end{aligned}
\tag{7}
$$

C_0 is a constant, such that at post-fault equilibrium point, the total energy, Eq. (7), is equal to zero. More details about energy function are given in [12], [13]. As it could be shown, the time derivative of the direct Lyapunov function Eq. (7) across the trajectories of the uncontrolled system is written by:

$$
\begin{aligned}
&\dot{w}(x) = -\sum_{k=1}^{M} D_k \omega_k^2 -\\
&-\sum_{k}^{M} \frac{T'_{dok}}{x_{dk} - x'_{dk}} (\dot{E}'_{qk})^2 \leq 0.
\end{aligned}
\tag{8}
$$

STATCOM supports grid voltage by exchanging reactive power with power system, which means the output voltage of VSI ($\bar{V}_{sh}$) is in phase with linked bus voltage ($\bar{V}_i$). But if dc-bus voltage (V_{dc})could be supported by an energy storage system, the VSI voltage angle (θ_{dc}) can varies from 0 to 2π and satisfies the condition of active power exchange.

Therefore STATCOM could be modeled as ideal voltage source and transformer leakage reactance x_{sh} in series (Fig. 3). Assume STATCOM/SMES is connected to bus i and its voltage amplitude relates to V_i by r_{sh}. Thus, VSI voltage is described as in Eq. (9).

$$
\begin{aligned}
&\bar{V}_{sh} = r_{sh} V_i e^{j\theta_{sh}} = V_i [r_{sh} \cos(\theta_{sh}) +\\
&j r_{sh} \sin(\theta_{sh})].
\end{aligned}
\tag{9}
$$

This voltage in synchronous reference frame has been explained as direct and quadrature component by Eq. (10):

$$
\bar{V}_{sh} = r_{sh} V_i e^{j\theta_{sh}} = V_i [u_d + j u_q]. \tag{10}
$$

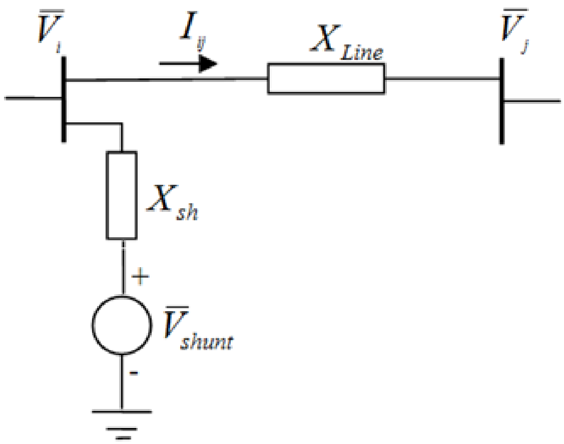

Fig. 3: Equivalent circuit of STATCOM.

STATCOM/SMES existence into the power system will modify the load flow Eq. (5) and also time derivative of Lyapannov function Eq. (5) will be changed. The powers equilibrium in i^{th} bus is based on Eq. (11):

$$
\begin{aligned}
&P_i + P_{Li} - P_{Gi} + P_{shi} = 0,\\
&Q_i + Q_{Li} - Q_{Gi} + Q_{shi} = 0,
\end{aligned}
\tag{11}
$$

where P_{shi} and Q_{shi} are interchanging active and reactive powers Between i^{th} bus and STATCOM/SMES consequently, which have been stated by Eq. (12):

$$
\begin{aligned}
&P_{shi} = b_{sh} V_i^2 [u_d \sin(\theta_i) - u_q \cos(\theta_i)],\\
&Q_{shi} = b_{sh} V_i^2 [1 - u_q \sin(\theta_i) - u_d \cos(\theta_i)],\\
&b_{sh} = 1/X_{sh}.
\end{aligned}
\tag{12}
$$

Time derivative of Lyapunov function with STATCOM/SMES existence is related to Eq. (13):

$$
\dot{w} = \dot{w}_{uncontrol} - P_{shi}\dot{\theta}_i - Q_{shi}\frac{\dot{V}_i}{V_i}. \tag{13}
$$

Based on Eq. (13), it is obvious that by controlling the inputs the negative rate of Lyapanov function will be increased. Controlling parameters (u_d, u_q) consist in transient (u''_d, u''_q) and steady-state controlling components (u'_d, u'_q), which have large time constant and improving system dynamic behavior extremely effective, Thus just single transient components are considered for power oscillation damping. By replacing Eq. (12) in Eq. (13) and set them based on controlling parameters, Eq. (14) will be gained:

$$\begin{aligned}\dot{w} &= \dot{w}_{uncontrol} - b_{sh}V_i\frac{d}{dt}[-V_i\cos(\theta_i)]u''_d- \\ &-b_{sh}V_i\frac{d}{dt}[-V_{i\,\sin(\theta_i)}]u''_g.\end{aligned} \tag{14}$$

$\bar{V}_i$ is written into the synchronous reference frame as:

$$\bar{V}_i = V_i\cos(\theta_i) + jV_i\sin(\theta_i) = V_{di} + jV_{qi}. \tag{15}$$

By replacing Eq. (15) in Eq. (14), the Eq. (16) will be gained:

$$\begin{aligned}\dot{w} &= \dot{w}_{uncontrol} - b_{sh}V_i\frac{d}{dt}(-V_{di})u''_d- \\ &-b_{sh}V_i\frac{d}{dt}(-V_{qi})u''_g.\end{aligned} \tag{16}$$

In order to keep negative sign in Eq. (16), transient controlling components (u''_d, u''_q) should have a similar sign with their sign of coefficients. Therefore STATCOM controlling law that has been derived from Eq. (16) will be as in Eq. (17):

$$\begin{aligned}u''_d &= k_1\frac{d}{dt}(-V_{di}), \\ u''_g &= k_2\frac{d}{dt}(-V_{gi}),\end{aligned} \tag{17}$$

where k_1 and k_2 are positive coefficients and their value depends on oscillation damping time. In order to decentralize control strategy, all of the measurement signals must be local. On the other hand due to obtained control strategy from Eq. (17) a reference frame signal, that should be a local signal is required. If V_i consider in a reference frame, u''_q will became zero in Eq. (17) and in this case Lyapanov method wouldn't be an optimum strategy, so we consider I_{ij} to provide synchronous reference frame in order to calculate the direct-axis and quadrature-axis components of ac voltage bus and converter voltage and provides a complete decentralized control law.

$$\begin{aligned}&P_{shi} = b_{sh}V_i(u'_dV_{qi} - u'_qV_{di}) = 0, \\ &u'_dV_{qi} - u'_qV_{di}) = 0.\end{aligned} \tag{18}$$

The voltage error value $(V_{refi} - V_i)$ is given to PI-controller to generate control signal (λ'_{qsh}) which is related to STATCOM reactive power. Thus, following equations could be defined:

$$\begin{aligned}&V_i - u'_dV_{di} - u'_qV_{qi} = \lambda'_q, \\ &u'_dV_{di} + u'_qV_{qi} = \lambda_q, \\ &\lambda_q = V_i - \lambda'_q.\end{aligned} \tag{19}$$

From Eq. (18) to Eq. (19) the control parameters for steady-state could be present as Eq. (20):

$$\begin{aligned}u'_d &= \frac{\lambda_qV_{di}}{(V_{qi})^2 + (V_{di})^2} = \frac{\lambda_qV_{di}}{V_i^2}, \\ u'_q &= \frac{\lambda_qV_{qi}}{(V_{qi})^2 + (V_{di})^2} = \frac{\lambda_qV_{qi}}{V_i^2}.\end{aligned} \tag{20}$$

4. Simulation Results

The effectiveness of the proposed control strategy will be illustrated using a three-machine test system in PSCAD/EMTDC software [14]. A single line of a sample system diagram has been demonstrated in figure 4. In this system, Generator G_3 has high power and consider as an infinite bus. Generators G_1 and G_2 have different inertial constant, hence system reveal similar behavior like actual power systems. A temporary short circuit occurred in bus 5 (B_5) while a STATCOM/SMES compensator placed in line 4 (L_4). In this simulation a unit SMES (100MJ/10H) have been utilized. The System responses with and without STATCOM/SMES presence are shown.

4.1. Without Compensation

The characteristics related to variation in speed, active and reactive power of generator G_1 have been represented in Fig. 5, Fig. 6 and Fig. 7, respectively. According to these characteristics, it can be seen that during sampling, all characteristics were in oscillation states and they are not damped.

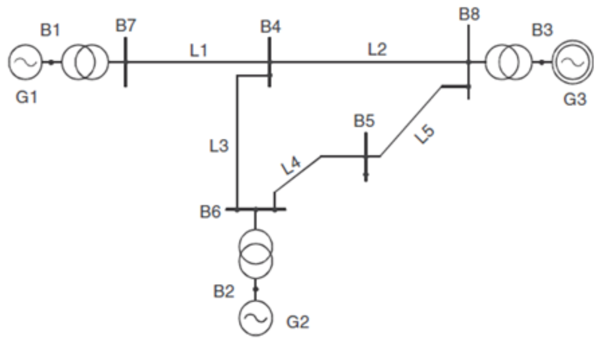

Fig. 4: Three-machine test system.

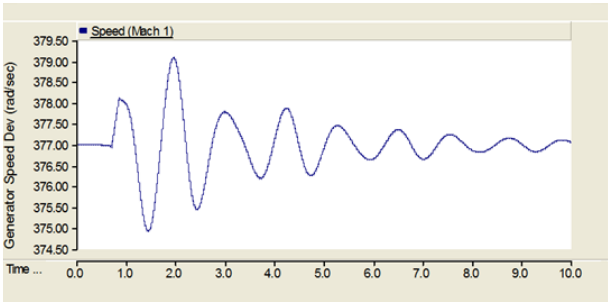

Fig. 5: Generator No.1 speed without compensation presence.

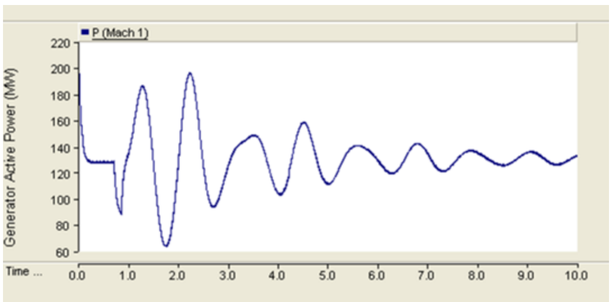

Fig. 6: Generator No.1 active power without compensation presence.

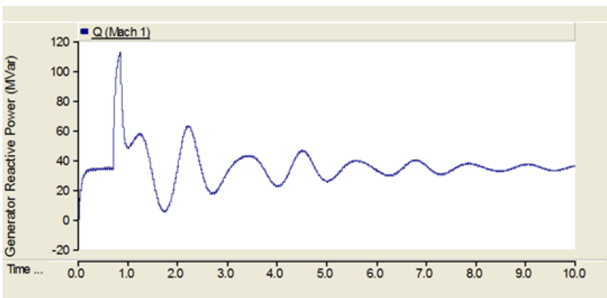

Fig. 7: Generator No.1 reactive power without compensation presence.

4.2. With STATCOM/SMES Compensator

Now in this condition, STATCOM/SMES compensator has been put in the bus5 B_5 of test system. Generator G_1 active power deviations have been represented in Fig. 9, as it can be seen under this conditions, oscillations amplitude of power in comparison to previous state decrease rapidly and this fluctuation have been damped and also these oscillations are damped in less time. Generator G_1 speed and reactive power variation characteristics have been shown in Fig. 8 and Fig. 10 respectively, that expresse desirable performance of STATCOM/SMES combinational compensation is in damping oscillations and increasing system safety and improvement in dynamic performance of power system.

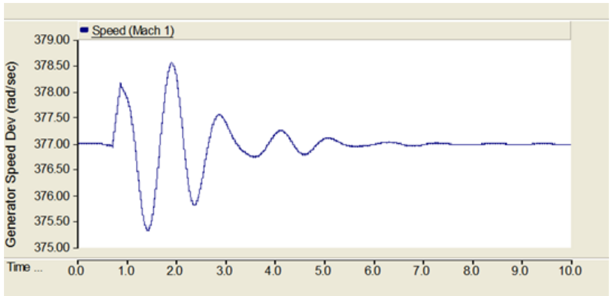

Fig. 8: Generator No.1 speed with STATCOM/SMES compensator presence.

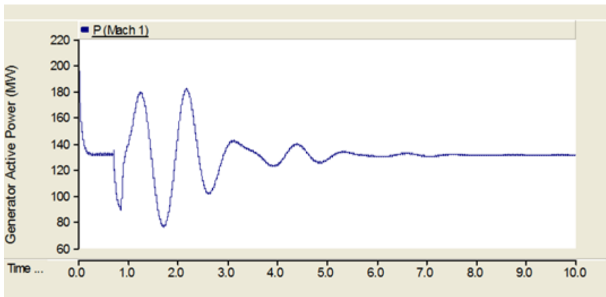

Fig. 9: Generator No.1 active power with STATCOM/SMES compensator presence.

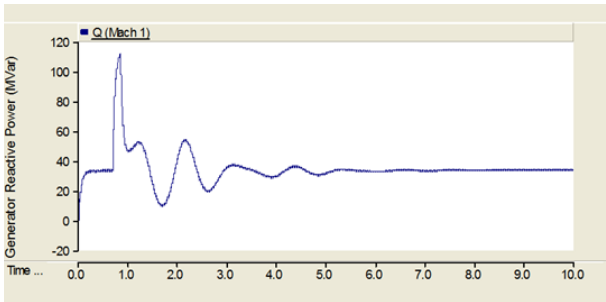

Fig. 10: Generator No.1 reactive power with STATCOM/SMES compensator presence.

4.3. Overload in Bus 6 (B_6)

In this case, regarding to short circuit which occurred in system, a 100 MW and 6.6 MVAR load have been place in bus 6 B_6. Simulation results related to speed and active power deviations of generator G_1 have been represented in Fig. 11 and Fig. 12, respectively. Now STATCOM/SMES compensator have been placed in the bus5 B_5 of test system, characteristics of generator G_1 have been represented in Fig. 13 and Fig. 14, respectively. By comparison between specification in two state of with and without compensator it can be seen that integrated compensator have a significant effect on power oscillation damping, while the first oscillation damping have been decreased by presence of STATCOM/SMES compensator.

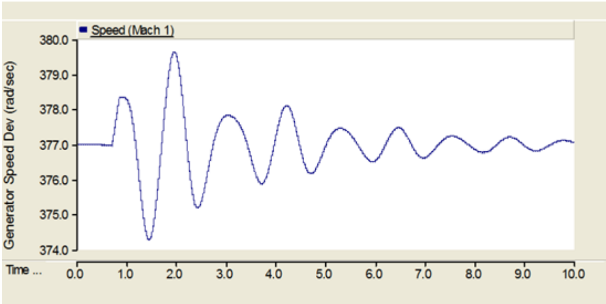

Fig. 11: Generator No.1 speed in state of overload in system and without compensation.

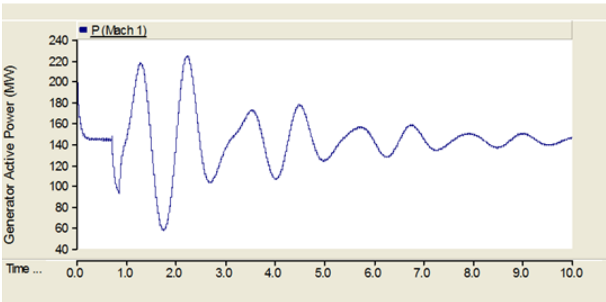

Fig. 12: Generator No.1 active power in state of overload in system and without compensation.

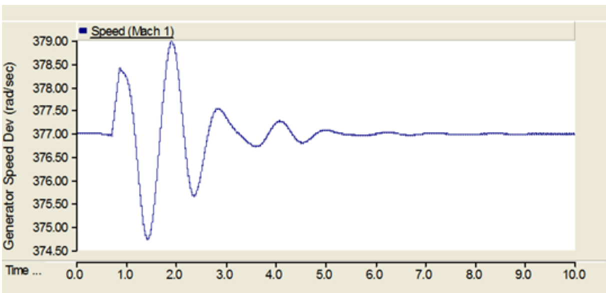

Fig. 13: Generator No.1 speed in state of overload in system and with STATCOM/SMES compensator presence.

4.4. Change in SMES Capacity

In the simulation which have been done in sections 4.1, 4.2 and 4.3 a unit SMES (10H) coil have been used, now we put a unit SMES (12H) coil and we expect that by

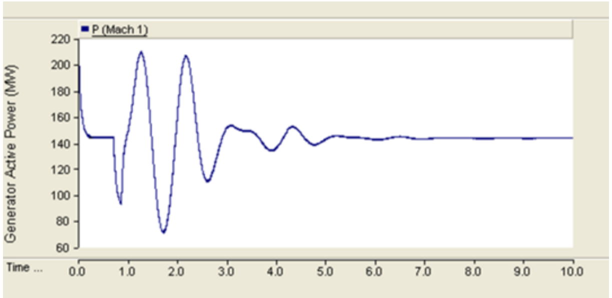

Fig. 14: Generator No.1 active power in state of overload in system and with STATCOM/SMES compensator presence.

increasing SMES coil capacity according to equation $E = \frac{1}{2}LI^2$ the stored energy in coil increase and as a result more energy transfer will occurr in system. On the other hand, since transient and dynamic stability are significantly control by active power and SMES storage transfers active power therefore it expects that increasing in storage capacity leads to improvement of power system dynamic operation. Simulation results related to generator G_1, active and reactive power characteristics have been demonstrated in Fig. 15 and Fig. 16, respectively.

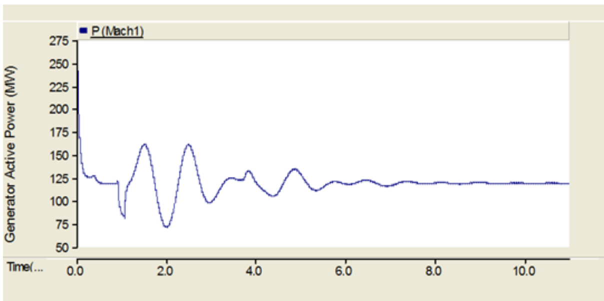

Fig. 15: Generator No.1 active power in state of SMES capacity variation.

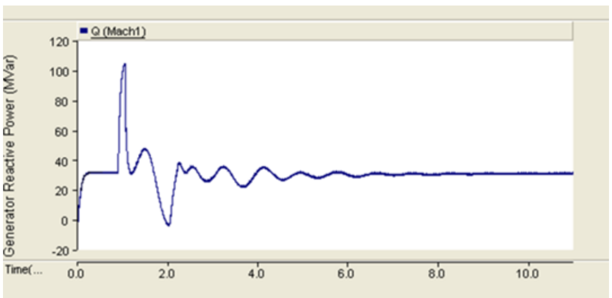

Fig. 16: Generator No.1 reactive power in state of SMES capacity variation.

5. Conclusion

This paper presents the specifications and operation of integrated STATCOM/SMES compensator. Also, a benefit of integration of SMES system into STATCOM was presented. Integrated STATCOM/SMES compensator would have the ability to independently and simultaneously, exchange both real and reactive power with a transmission system. The simulation results show that STATCOM/SMES compensator has a more significant effect on dynamic performance improvement.

References

[1] UZUNOVIC, E. *Transient Stability and Power Flow Models of VSC FACTS controllers.* Waterloo, 2001. Ph.D. dissertation thesis. University of Waterloo.

[2] GLANZMANN, G. *FACTS, Flexible Alternating Current Transmission Systems.* Zurich: EEH-Power Systems Laboratory, 2005. DOI: 10.3929/ethz-a-004891251.

[3] TYLL, H. K. FACTS technology for reactive power compensation and system control. In: *2004 IEEE/PES Transmision and Distribution Conference and Exposition: Latin America.* Sao Paulo: IEEE, 2004, pp. 976–980. ISBN 0-7803-8775-9. DOI: 10.1109/TDC.2004.1432515.

[4] PULESTON, P. F., S. A. GONZALEZ and F. VALENCIAGA. A STATCOM based variable structure control for power system oscillations damping. *International Journal of Electrical Power.* 2007, vol. 29, iss. 3, pp. 241–250. ISSN 0142-0615. DOI: 10.1016/j.ijepes.2006.07.003.

[5] RAO, P., M. L. CROW and Z. YANG. STATCOM control for power system voltage control applications. *IEEE Transactions on Power Delivery.* 2000, vol. 15, iss. 4, pp. 1311–1317. ISSN 0885-8977. DOI: 10.1109/61.891520.

[6] TAN, Y. L. and Y. WANG. A robust nonlinear excitation and SMES controller for transient stabilization. *International Journal of Electrical Power.* 2004, vol. 26, iss. 5, pp. 325–332. ISSN 0142-0615. DOI: 10.1016/j.ijepes.2003.10.017.

[7] ZHANG, L., C. SHEN, M. L. CROW, L. DONG, S. PEKAREK and S. ATCITTY. Performance Indices for the Dynamic Performance of FACTS and FACTS with Energy Storage. *Electric Power Components and Systems.* 2004, vol. 33, iss. 3, pp. 299–314. ISSN 1532-5016. DOI: 10.1080/15325000590474438.

[8] YANG, Z., C. SHEN, L. ZHANG, M.L. CROW and S. ATCITTY. Integration of a StatCom and battery energy storage. *IEEE Transactions on Power Systems.* 2001, vol. 16, iss. 2, pp. 254–260. ISSN 0885-8950. DOI: 10.1109/59.918295.

[9] ARSOY, A., Y. LIU, P. F. RIBEIRO and F. WANG. Power converter and SMES in controlling power system dynamics. In: *Industry Applications Conference, 2000. Conference Record of the 2000 IEEE.* Rome: IEEE, 2000, pp. 2051–2057. ISBN 0-7803-6401-5. DOI: 10.1109/IAS.2000.883109.

[10] JOHNSON, B. K. and H. L. HESS. *Incorporating SMES Coils into FACTS and Custom Power Devices.* Moscow, 2000. University of Idaho. Available at: `http://www.ee.uidaho.edu/ee/power/brian/PAPERS/smesapp.pdf`.

[11] GYUGYI, L., Y. LIU, P. F. RIBEIRO and F. WANG. Application characteristics of converter-based FACTS controllers. In: *2000 International Conference on Power System Technology.* Perth: IEEE, 2000, pp. 391–396. ISBN 0-7803-6338-8. DOI: 10.1109/ICPST.2000.900089.

[12] GHANDHARI, M.. *Control Lyapunov Function: A Control Strategy for Damping of Power Oscillations in Large Power Systems.* Stockholm, 2000. Ph.D. Dissertation thesis. Royal Institute of Technology.

[13] JANUSZEWSKI, M., J. MACHOWSKI and J. W. BIALEK. Application of the direct Lyapunov method to improve damping of power swings by control of UPFC. *IEE Proceedings - Generation, Transmission and Distribution.* 2004, vol. 151, iss. 2, pp. 252–260. ISSN 1350-2360. DOI: 10.1049/ip-gtd:20040054.

[14] Manitoba HVDC Research Center, *PSCAD/EMTDC User's Manual.* Manitoba, 1988. Available at: `https://hvdc.ca/uploads/ck/files/reference_material/EMTDC_User_Guide_v4_2_1.pdf`.

About Authors

Mahmoud Reza SHAKARAMI was born in Khorramabad, Iran, in 1972. He received his M.Sc. and Ph.D. degree in Electrical Engineering from Iran University of Science and Technology of Tehran, Tehran, Iran, in 2000 and 2010 and is currently an Assistant Professor in Electrical Engineering Department of Lorestan University, Lorestan, Iran. His current

research interests are: power system dynamics and stability and FACTS devices.

Reza SEDAGHATI was born in Kazeroon, Iran, on September 21, 1983. He received his M.Sc. degree in Electrical Engineering in 2009. He is currently as a Ph.D. student in Department of Electrical Engineering of Lorestan, Lorestan, Iran. His research interests include renewable energies, optimization, FACTS devices and power system dynamics.

Mohammad Bagher HADDADI was born in Shiraz, on September 1, 1988. He received his B.Sc. degree in Electrical Engineering from Shahid Beheshti University, Tehran, Iran, in 2011 and M.Sc. degree in Electrical Engineering from the university of Shiraz, Shiraz, Iran in 2013. His research interests also include power electronic, digital signal processing in optoelectronics and radiation protection.